

# Investigating the Formation of ‘Molybdenum Blues’ with Gel Electrophoresis and Mass Spectrometry

Ippei Nakamura,<sup>†</sup> Haralampos N. Miras,<sup>§</sup> Aya Fujiwara,<sup>‡</sup> Masaru Fujibayashi,<sup>‡</sup> Yu-Fei Song,<sup>⊥</sup> Leroy Cronin<sup>\*§</sup> and Ryo Tsunashima<sup>\*†</sup>

<sup>†</sup>Graduate School of Science and Engineering, Yamaguchi University, Yamaguchi, 753 8512, Japan.

<sup>‡</sup>Department of biology and chemistry, Yamaguchi University, Yamaguchi, 753 8512, Japan.

<sup>§</sup>School of Chemistry, University of Glasgow, Glasgow, UK.

<sup>⊥</sup>State Key Laboratory of Chemical Resource Engineering, Beijing University of Chemical Technology, 100029 Beijing, P. R. China.

**KEYWORDS.** Polyoxometalates, Self-assembly, Systems chemistry, Electrophoresis, Mass spectrometry

**ABSTRACT:** The reduction of solutions of acidified molybdate leads to the formation of a family of nanostructured molybdenum blue (MB) wheels which are linked together in a series of complex reaction networks. These networks are complex because the species which define the nodes are extremely labile, unstable, and common to many different networks. Herein, we combine gel electrophoresis and electrospray ionization mass spectrometry (ESI-MS) to investigate the effect of the pH and the ratio of reactants and reducing agents, R ( $R = [S_2O_4^{2-}]/[MoO_4^{2-}]$ ), on the complex underlying set of equilibria that make up MBs. By mapping the reaction parameter space given by experimental variables such as pH, R, solvent medium, and type of counterion, we show that the species present range from nanostructured MB wheels (comprising ca. 154 Mo atoms) to smaller molecular capsules,  $[(SO_3)_2MoV_2MoVI_6O_{54}]^{6-}$  ( $\{S_2Mo_8\}$ ), and templated hexameric  $[(\mu_6-SO_3)MoV_6O_{15}(\mu_2-SO_3)_3]^{8-}$  ( $\{S_4Mo_6\}$ ) anions. The parallel effects of templation and reduction on the self-assembly process are discussed, taking into consideration the Lewis basicity of the template, the oxidation state of the Mo centers, and the polarity of the reaction medium. Finally, we report a new type of molecular cage (TBA)<sub>5</sub>[Na(SO<sub>3</sub>)<sub>2</sub>(PhPO<sub>3</sub>)<sub>4</sub>MoV<sub>4</sub>MoVI<sub>14</sub>O<sub>49</sub>]-nMeCN (1), templated by SO<sub>3</sub><sup>2-</sup> anions and decorated by organic ligands. This discovery results from the exploration of the cooperative effect of two anions possessing comparable Lewis basicity, and we believe this constitutes a new synthetic approach for the design of new nanostructured molecular metal oxides and will lead to a greater understanding of the complex reaction networks underpinning the assembly of this family of nanoclusters.

## 1. INTRODUCTION

Solutions of molybdenum blues (MBs),<sup>1</sup> first mentioned by Scheele in 1783, comprise a family of nanostructured polyoxometalate (POM) clusters<sup>2</sup> where their deep-blue color originates from the partial reduction of MoVI centers to MoV giving a delocalized mixed valence state. Their preparation is achieved by the partial reduction of solutions of acidified molybdate(VI). Crystallization of the solutions lead to isolation of particular species, the nature of which is precisely defined by the pH of the reaction mixture. Specifically, acidification of Na<sub>2</sub>MoO<sub>4</sub> aqueous solution (12.7 mM, 25 mL) with hydrochloric acid (32%, 2.7 mL, results in solution pH ≈ 1) and consecutive reduction by Na<sub>2</sub>S<sub>2</sub>O<sub>4</sub> (0.15 g, 0.86 mmol) leads to the formation of a nanostructured, wheel-shaped, Mo-oxide cluster composed of 154 (152) Mo atoms bridged by O atoms after 1–2 days.

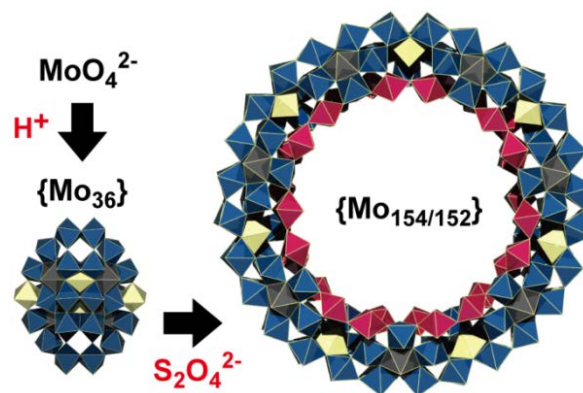


**Figure 1.** Schematic view of the formation of the {Mo<sub>154/152</sub>} wheel. The polyhedral building blocks are colored as follows: {Mo<sub>1</sub>}, yellow; {Mo<sub>2</sub>}, red; {Mo<sub>8</sub>}, blue with a black pentagonal central group.

The mixed valence wheel is reduced by 28 electrons with a formula of  $\text{Na}_{15}[\text{Mo}_{154}\text{O}_{462}\text{H}_{14}(\text{H}_2\text{O})_{70}]_{0.5}[\text{Mo}_{152}\text{O}_{457}\text{H}_{14}(\text{H}_2\text{O})_6]_{0.5} \cdot \text{ca.}400\text{H}_2\text{O}$  ( $= \text{Na}_{15}\{\text{Mo}_{154}/152\} \cdot \text{ca.}400\text{H}_2\text{O}$ ).<sup>3</sup> The structure can be rationalized simply by grouping the individual metal-centered units into building blocks, namely:  $14 \times$  each of  $\{\text{Mo}_1\}$ ,  $\{\text{Mo}_2\}$ , and  $\{\text{Mo}_8\}$  (Figure 1). Furthermore, the controlled elimination of  $\{\text{Mo}_2\}$  building units leads to the formation of similar wheels with “defect” sites where the wheel is formulated as  $\{\text{Mo}_{154-x}\}$  ( $x = 0-16$ ).

This family of compounds does attract attention due to their structural complexity and their interesting behavior in solution. For example, Liu et al. revealed that the  $\{\text{Mo}_{154}/152\}$  wheels form assemblies that have a vesicle-like or “blackberry” structure in solution even though they do not possess amphiphilic characteristics, which are often crucial for the formation of such assemblies. Investigation of the systems reveals that the electrostatic interactions between the clusters and counterions are necessary for the formation of vesicles.<sup>4</sup> Additionally, a variety of applications, owing to the reactivity of the nanowheel, was proposed in areas such as catalysis, ion conduction, and host-guest chemistry.<sup>5</sup> Apart from these interesting properties, the complex formation mechanism attracted the attention of several research groups. Recently, the use of continuous flow reactors allowed the controlled reduction of the reaction mixture, giving the opportunity to isolate and characterize crystallographically an intermediate species of the MB family where the  $\{\text{Mo}_36\}$  cluster templates the formation of the MB wheel (Figure 1).<sup>6</sup>

In general, isolation of POM clusters has been achieved by crystallization, which requires precise control of both reaction and crystallization conditions as well as appropriate selection of cations and solvents. Occasionally, the inability to isolate single crystals from a reaction mixture leads to ambiguity with respect to the structure of the compound(s) isolated. This is due to the inherent difficulty of analyzing such complex mixtures. For example the majority of the MB species have similar solubility and absorption in UV-vis-NIR region, making the direct probing of the speciation of the reaction mixture practically impossible. Recently, we demonstrated that gel electrophoresis is a powerful technique for the characterization of reaction mixtures containing POM clusters.<sup>7</sup> This is because they have a unique electrophoretic mobility depending on their size and charge (surface charge density) in solution. Initial analysis of the reaction mixture using gel electrophoresis allowed us to investigate and identify the species formed in the reaction mixture.

In this paper, we present our investigations into the MB reaction mixture as a function of pH and reagents ratio (R) and map the reaction coordinates that define and control the system. The extent of reduction on the metal centers as well as the pH of the reaction mixture and type of counteraction is crucial for the formation of either MB species or a variety of other anionic clusters, as we confirmed by gel electrophoretic chromatography and ESI-MS studies. Thus, mapping the parameter space in respect of experimental variables such as pH, R, solvent

medium, and counterion effects, we identified the formation of species ranging from nanostructured MB wheels to molecular capsules  $[(\text{SO}_3)_2\text{MoV}_2\text{MoVI}_6\text{O}_{54}]_6 - (= \{\text{S}_2\text{Mo}_{18}\})$  and hexameric anionic  $[(\mu_6\text{-SO}_3)\text{MoV}_6\text{O}_{15}(\mu_2\text{-SO}_3)_3]_8^- (= \{\text{S}_4\text{Mo}_6\})$  clusters. The interplay of Lewis basicity of the heteroatom present and its ability to template the self assembly of building blocks proved crucial for the isolation of specific products. Experimental observations suggest: (a) strong Lewis base behavior of the anionic species, (b) a lower oxidation state of Mo, and (c) low polarity of the solvent medium favors the templated self-assembly process. For example, use of  $\text{SO}_3^{2-}$  as a template (originating from the oxidation of the reductant  $\text{Na}_2\text{S}_2\text{O}_4$ ) allowed us to isolate a Dawson-like  $\{\text{S}_2\text{Mo}_{18}\}$  and a hexameric anionic species  $\{\text{S}_4\text{Mo}_6\}$  in the presence of mixed solvent system (acetonitrile:- water) and tetrabutylammonium (TBA) cations. This observation allowed us to develop a new synthetic approach for the design of new types of clusters. Based on the above approach, the use of  $\text{SO}_3^{2-}$  and phenylphosphonate anions in a mixed solvent system allowed the isolation of new molecular capsule  $(\text{TBA})_5[\text{Na}(\text{SO}_3)_2(\text{PhPO}_3)_4\text{MoV}_4\text{MoVI}_{14}\text{O}_{49}] \cdot n\text{MeCN}$  (1), where the sulfite anions occupy the interior cavities and the external surface is decorated by four phosphonate ligands. This cluster itself represents a new archetype.

## 2. RESULTS AND DISCUSSION

### 2.1 Molybdenum-blue and Molybdenum-brown

The system was investigated as a function of pH and the ratio of the starting materials ( $R = [\text{S}_2\text{O}_4^{2-}]/[\text{MoO}_4^{2-}]$ ).

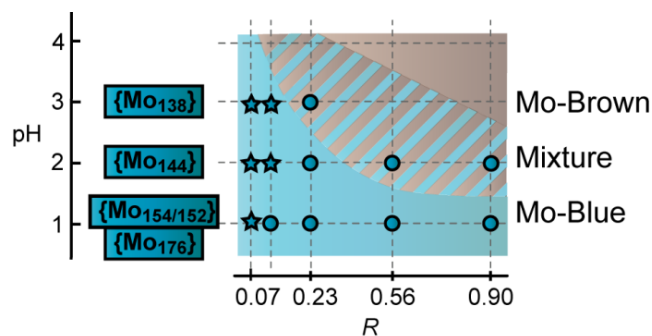


**Figure 2.** Diagram of Mo-blue and Mo-brown in solution. Circles and stars show the conditions that yield MB-wheels, but conditions that lead to single crystals are denoted by the stars.

A series of reaction mixtures under different experimental conditions of pH (1-4) and R (0.07, 0.14, 0.23, 0.56 and 0.9), were characterized by UV-vis-NIR spectroscopy (figure S1-1 to S1-6). The MB species have typical absorption bands around at 600-1100 nm which are attributed to the inter-valence charge transfer (IVCT). Similar bands were observed for all the combinations of experimental conditions (pH, R) except from the sets (3, 0.90) and (4, 0.56-0.90). Under these experimental conditions the reactions mixtures appeared to be brown instead of blue due to the higher amount of reducing agent, which lead to the formation of Mo-Brown species.<sup>1</sup>

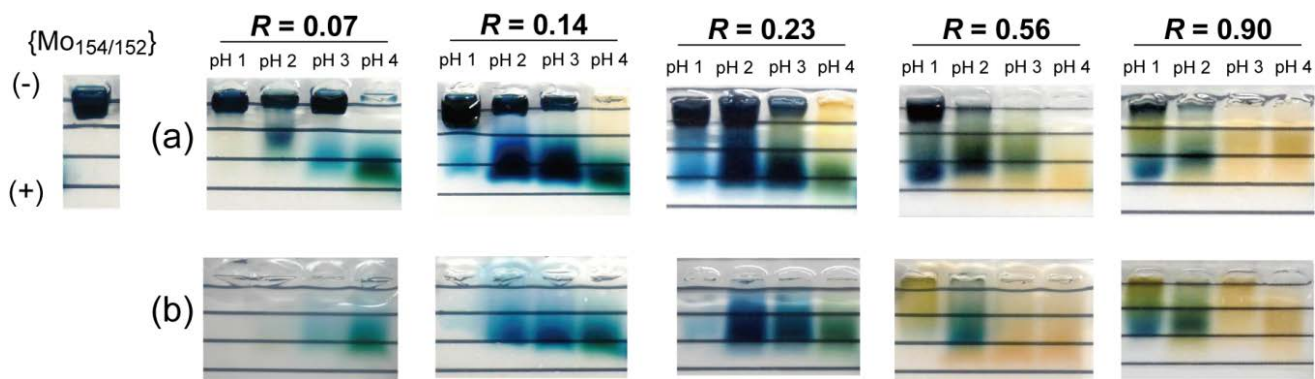


**Figure 3.** Photograph of gels after electrophoresis of (a) filtrates after reactions and (b) filtrates after treatment of TEAH (taken at 10 min of the run). In the gels shown in (b), blue bands that have slowest mobility were diminished if compared with initial solution shown figure (a). Comparable mobility of the blue band with  $\{\text{Mo}_{154/152}\}$  and IR spectra of TEAH salt indicate separation of MB-wheels.

The UV-vis-NIR data allowed us to identify the areas of the parameter space that lead to the formation of MB and the areas of Mo-brown species [(3, 0.90) and (4, 0.56-0.90)] (figure 2). The area of the parameter space which favors the formation of Mo-brown species was partially contaminated with MB species as confirmed by chromatographic gel-electrophoresis (see below for further details). After leaving the reaction mixtures to stand at room temperature for 3 days, single crystals were obtained from the (1, 0.07) and (2, 0.07-0.14) reaction sets. Single crystal X-ray diffraction analysis, revealed two cluster types within the reaction mixture at (1, 0.07);  $\text{Na}_{15}\{\text{Mo}_{154/152}\}\cdot\text{ca.}400\text{H}_2\text{O}$  and  $\text{Na}_{16}[\text{Mo}_{176}\text{O}_{528}\text{H}_{16}(\text{H}_2\text{O})_{86}]\cdot\text{ca.}450\text{H}_2\text{O}$  ( $[\text{Mo}_{176}\text{O}_{528}\text{H}_{16}(\text{H}_2\text{O})_{86}]^{16-} = \{\text{Mo}_{176}\}$ ).<sup>8</sup> From the reaction set (2, 0.07-0.14), single crystals of  $\text{Na}_{24}\{[\text{Mo}_{144}\text{O}_{437}\text{H}_{14}(\text{H}_2\text{O})_{56}]_{0.5}[\text{Mo}_{144}\text{O}_{437}\text{H}_{14}(\text{H}_2\text{O})_{60}]_{0.5}\}\cdot 350\text{H}_2\text{O}$  ( $= \{\text{Mo}_{144}\}$ )<sup>9</sup> were obtained. Finally, the reaction sets (3, 0.07-0.14) gave single crystals after 24 hrs when treated with ammonium chloride. The cluster was crystallographically identified as  $[\text{Mo}_{138}\text{O}_{410}(\text{OH})_{20}(\text{H}_2\text{O})_{46}]^{40-}$  ( $= \{\text{Mo}_{138}\}$ )<sup>10</sup>.

## 2.2 Chromatographic gel-electrophoresis and mass spectroscopic analysis of reaction solutions

Although reaction sets (1-3, 0.07) and (2-3, 0.14) gave single crystals, it was possible to identify the species in solution in the other collected batches using gel-electrophoresis. Figure 3 shows the photograph of gels taken after the electrophoresis of the reaction mixtures after one day of reaction. The reaction set (1, 0.07) gave a single blue band, implying there is only a single product attributable to a MB-species. The reaction conditions used are consistent with the synthesis of the  $\{\text{Mo}_{154/152}\}$  anions (The MB wheel,  $\{\text{Mo}_{154/152}\}$ , was synthesized from a  $\text{Na}_2\text{MoO}_4$  aqueous solution in the presence of  $\text{Na}_2\text{S}_2\text{O}_4$  reducing agent at  $\text{pH} \approx 1$ , yielding blue crystals after 2 days).

On the other hand, solutions from the reaction mixtures that did not crystallize were separated into several bands corresponding to species with different electrophoretic mobility and colours (blue, green and brown). As such, we revealed that Mo-brown was a contaminant in reactions (4, 0.14), (3-4, 0.23), (2-4, 0.56) and (2-4, 0.90).

Mass spectroscopy of several reaction sets revealed very complex spectra with multiple complex envelopes that show a wide isotopic distribution, as expected for large MB anions. Only three types of cluster anions:  $[\text{Mo}_4^{\text{VI}}\text{O}_{13}\text{Na}]^-$ ,  $[\text{Mo}_4^{\text{V}}\text{O}_{14}\text{H}_7]^-$  and  $[\text{Mo}_4^{\text{VI}}\text{O}_{13}\text{H}]^-$  could be assigned (Figure 4). These cluster anions have been observed as building blocks that exist in reaction systems.<sup>11</sup> Most of other species could not be assigned to known cluster types. We deduce that these species contain other building blocks or fragments of clusters that possess mixed valence state molybdenum centres, as suggested by IVCT signals in UV-vis-NIR spectra. Our mass spectroscopic analysis of the reaction solutions indicated that (i) reactions did not yield single cluster anions and (ii) reaction solutions contain mixtures of clusters including building blocks and fragments that have not been isolated as crystalline forms.

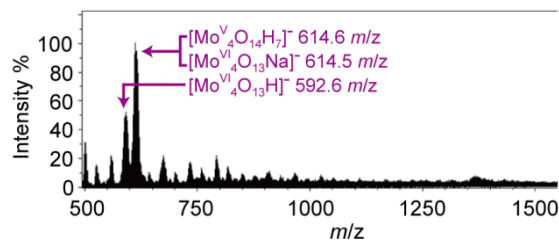


**Figure 4.** ESI-MS spectrum of solution reacted at (3, 0.14).

## 2.3 Construction of reaction diagrams of MB-wheels

Isolation of MB-material was achieved by the reaction with TEAH chloride. Upon treatment by TEAH chloride, a blue precipitate was immediately observed from reactions (1-3, 0.07-0.23) and (1-2, 0.56-0.9). The IR spectra of these blue powders showed a Mo-O-Mo vibration at around  $900\text{-}500\text{ cm}^{-1}$  and they were similar to  $\{\text{Mo}_{154/152}\}$  anion (figure S4-1 to S4-5). Figure 3b shows a photograph of gel after the electrophoresis of filtrates after separating the TEAH salts. All the blue bands that had the slowest mobility in the initial filtrates seen in reactions (1-3, 0.07-0.23) and (1-2, 0.56-0.9) had disappeared, showing isolation of MB-wheels as TEAH salts. By comparison of the

mobility data and IR spectra, it can be suggested that the MB-wheels are formed in reactions (1-3, 0.07-0.23) and (1-2, 0.56-0.9) as shown in figure 2. In addition, Ozeki reported that reaction pH effects to control the  $x$  value of  $\{\text{Mo}_{154-x}\}$  ( $x = 0-16$ ). Depending on reaction pH, lacunary gigantic MB-wheels were formed, where pH increase tend to cause increases in  $x$ .<sup>10</sup> As mentioned before, we also isolated  $\{\text{Mo}_{144}\}$  and  $\{\text{Mo}_{138}\}$  anions from reactions at pH 2 and 3 ( $R = 0.07-0.14$ ), respectively, showing a similar tendency with changing pH.

#### 2.4 Triggering template reactions from the building block mixture.

By focusing on the isolation of the building blocks, several sets of reaction yielded blue precipitates after treatment with TBA (reactions except for (3, 0.90) and (4, 0.56-0.90)). Recrystallization from acetonitrile yielded single crystals which were identified as the TBA salt of  $[\text{Mo}_2\text{Mo}_{16}\text{O}_{54}(\text{SO}_3)_2]^{6-}$  ( $\{\text{S}_2\text{Mo}_{18}\}$ )<sup>12</sup> by single crystal X-ray diffraction (XRD) analysis. This Dawson-like cluster has been reported earlier<sup>12</sup> in agreement with the employed reaction conditions, (4, 0.07) (while the concentration of  $\text{MoO}_4^{2-}$  differs). A diagram in which  $\{\text{S}_2\text{Mo}_{18}\}$  was obtained was shown in figure 4a.

Further, an increase of the pH and  $R$  parameters yielded orange crystals of the  $[(\mu_6\text{-SO}_3)\text{Mo}_6\text{O}_{15}(\mu_2\text{-SO}_3)_3]^{8-}$  ( $\{\text{S}_4\text{Mo}_6\}$ ) anion after two weeks.<sup>13</sup> The parameter space scanned for the isolation of the hexameric cluster is shown in figure 4b. The synthesis was reported using hydrazine and  $(\text{NH}_4)_2\text{SO}_3^{2-}$  as a reductant and template source, respectively. Reaction condition (pH,  $[\text{SO}_3^{2-}]/[\text{Mo}]$ ) is agreed with (5.5, 5.3). Large content of  $\text{SO}_3^{2-}$  was required for reaction.

Interestingly, both  $\{\text{S}_2\text{Mo}_{18}\}$  and  $\{\text{S}_4\text{Mo}_6\}$  clusters were not identified by mass spectra shown above, indicating that their self-assembly was triggered by the addition of TBA and acetonitrile after which the sulphite anion acted as template.

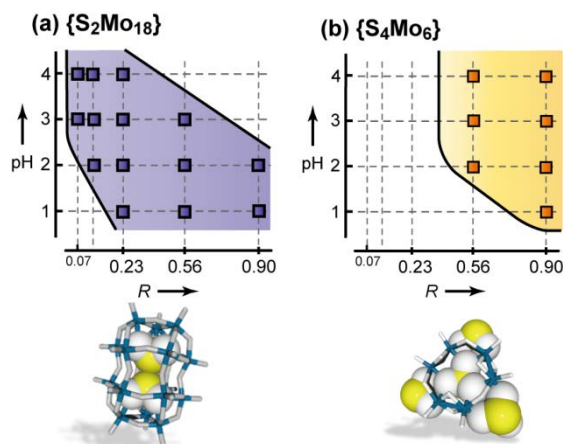


**Figure 4.** Diagrams and structures of  $\{\text{S}_2\text{Mo}_{18}\}$  and  $\{\text{S}_4\text{Mo}_6\}$  clusters (Mo: blue, O; white, S: yellow). Mo-oxide frameworks were represented by stick model with large spheres of  $\text{SO}_3^{2-}$ . Squares show the conditions that yield each cluster.

Also, the counter cation can play an important role and affect the self-assembly process.<sup>14</sup> Additionally, degradation of large species in solution giving rise to the formation of other species is also known, for example the fragmentation of the  $\{\text{Mo}_{132}\}$ -type gigantic cluster was observed following treatment with  $[\text{Cu}(\text{MeCN})_4]\text{PF}_6$ , which triggered the assembly of the inverse Keggin structure,  $[\text{Mo}_{12}\text{O}_{46}(\text{PF}_4)]^{4-}$ .<sup>15</sup>

#### 2.5 Template reactions of oxoanions.

It has long been known that  $\text{XO}_m^{n-}$  type oxoanions can act as templates in reactions, forming hetero-POMs. An important parameter which affects the ability of an anion to act as template is its Lewis basicity. The basic strength is correlated to the capacity of attracting protons. Thus, the basicity, that is the  $\text{p}K_a$  value of the corresponding anions, is correlated to the capacity to attract and interact with cationic species.

The Lewis base strength can be estimated from bond valence consideration as  $S_b$  and the values found to be in good agreement with the  $\text{p}K_a$  values of the specific anion ( $\text{p}K_a = 14.3 \ln(S_b/0.135)$ ).<sup>16</sup> Table 1 summarizes the  $\text{p}K_a$  and  $S_b$  values of different anions that were used as templates for the synthesis of hetero-POMs. If reaction solutions were treated with TBA·Br, followed by recrystallization in acetonitrile, these cluster anions were obtained as single crystals.

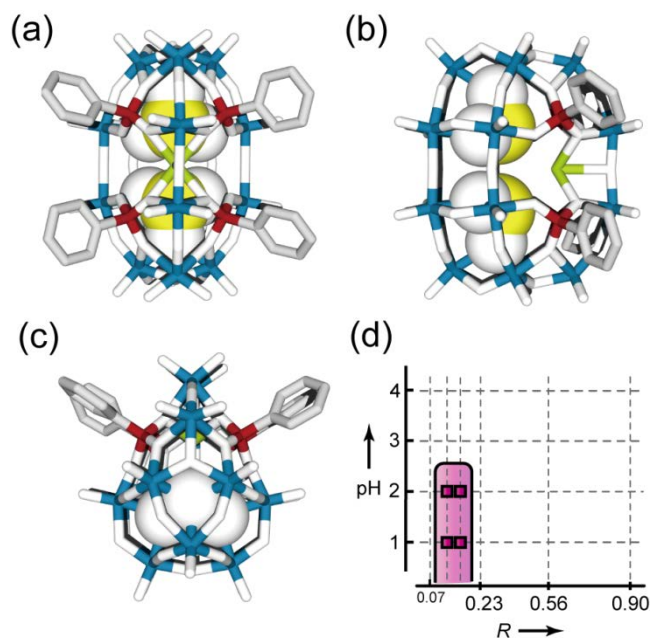


**Figure 5.** (a-c) Structure of  $[\text{Na}(\text{SO}_3)_2(\text{PhPO}_3)_4\text{Mo}^{\text{V}}_4\text{Mo}^{\text{VI}}_{14}\text{O}_{49}]^{5-}$  anion from different viewing directions with stick models in which  $\text{SO}_3^{2-}$  anions were highlighted by large ball representation (Mo; blue, O; white, P; red, C; grey, Na; green, S; yellow). H atoms were omitted. And, (d) diagram of the compound **1** (pH before adding acetonitrile) Squares show the conditions that yield cluster.

**Table 1.  $pK_a$  values and Lewis base strength<sup>a</sup> ( $S_b$ ) of corresponding anion of oxoacid summarized with reaction solvent for synthesis of hetero polyoxometalate clusters.**

anion	$pK_a^b$	$S_b$	Hetero-POM	Reaction solvent	Ref
$SiO_4^{4-c}$	~10	0.33	$[(SiO_4)(MoO_3)_{12}]^{4-}$	Water	18
$PO_4^{3-}$	12.3	0.25	$[(PO_4)(MoO_3)_{12}]^{3-}$	Water	19
$AsO_4^{3-}$	11.5	0.25	$[(AsO_4)(MoO_3)_{12}]^{3-}$ $[(AsO_4)(MoO_3)_{18}]^{6-}$	Water Water	19, 20
$B(OH)_4^-$	9.23	-	$[(BO_4)(WO_3)_{12}]^{5-}$	Water	19
$P_2O_7^{4-}$	9.25	0.22	$[(P_2O_7)(MoO_3)_{18}]^{4-}$	Water/acetonitrile	21
$SeO_3^{2-}$	8.3	0.22	$[Mo_{12}V_{10}O_{58}(SeO_3)_8]^{10-}$	Water	22
$TeO_3^{2-}$	8.0	0.22	$[Te_3W_{21}O_{75}]^{12-}$	Water	23
$SO_3^{2-}$	7.00	0.22	$[(SO_3)_2(MoO_3)_{18}]^{4-}$ $[(SO_3)_2W_{18}O_{62}]^{4-}$ $[(SO_3)_2(Mo^V O_3)_2(Mo^VI O_3)_{16}]^{6-}$	Water/acetonitrile Water/acetonitrile Water	12, 24
$MoO_4^{2-}$	3.89	0.17	-	-	-
$SO_4^{2-}$	1.9	0.17	$[(SO_4)(MoO_3)_{12}]^{2-}$ $[(SO_4)(MoO_3)_{18}]^{4-}$ $\{Mo_{368}\}^d$	Water/acetonitrile Water/acetonitrile Water	25
$ClO_4^-$	-10	0.08	$[(ClO_4)(W^V O_3)(W^VI O_3)_{17}]^{6-}$	DMF/acetic anhydride	26

<sup>a</sup>  $pK_a$  is correlated with  $S_b$ ;  $pK_a = 14.3 \ln(S_b/0.135)$  (see reference 16). <sup>b</sup>  $pK_a$  values see reference 27. <sup>c</sup> since the anion has not been isolated, shown in the table for comparison. <sup>d</sup>  $\{Mo_{368}\}$  ( $= [H_x Mo_{368} O_{1032} (H_2O)_{240} (SO_4)_{48}]^{48-}$ ) (see reference 25c; the cluster employs mixed valence state as seen in MB clusters and has partially encapsulated  $SO_4^{2-}$ . two or three O atoms of S were linked with Mo).

Reactions that exploit the template effect that different heteroatoms have on the formation of hetero-POM type molybdenum-blue clusters are used for routine colorimetric determinations of phosphates, silicates and arsenates. This originates from the high reactivity of these template anions towards the formation of hetero-POMs.<sup>17</sup> These oxoanions tend to have a high Lewis base strength and react readily with molybdate precursor in aqueous solution.

In contrast, hetero-POM encapsulating anions that are poor Lewis bases tend to be synthesized from mixed solvent systems and/or reducing conditions. In the case of the  $ClO_4^-$  anion, which has lowest base strength in the table, both a non-aqueous system and reducing conditions were required. This tendency indicates that mixed solvents and reducing conditions enhance reactivity. From bond valence considerations, the  $S_b$  of each template anion was estimated. In a model reaction with  $SO_3^{2-}$  as the template reacting with molybdate ions, the charge of Mo ions and Lewis base strength of O linked to S were denoted by  $m$  and  $S_b$ , respectively. The  $S_b$  is estimated as  $2-m/3$ . With a decrease in oxidation state (charge,  $m$ ) of Mo from 6 to 5,  $S_b$  is increased from zero to 0.17 (Figure S9-1).

This shows that the template reaction is easier under the reducing conditions and indicates that MB reactions are intrinsically pre-disposed to take part in templated self-assembly reactions.

## 2.6 Reaction with phenylphosphonate.

To exploit this understanding, we employed phenylphosphonate ( $PhPO_3^{2-}$ ) to explore the formation of a new cluster type. This is because the anion has similar Lewis base strength ( $pK_a$ , 1.86,  $pK_a$ , 7.51) to  $SO_3^{2-}$ , and we postulate that the steric hindrance by phenyl moiety can disturb the template reaction.<sup>28</sup> Therefore, to an aqueous solution of  $Na_2MoO_4 \cdot 2H_2O$  (12.6 mmol), we added hydrochloric acid (32 %),  $Na_2S_2O_4$  phenylphosphonic acid (3 mmol) where experimental variables pH and  $R$  tuned. Into the aqueous solutions, 10 mL of acetonitrile was mixed under continuous stirring (for 30 minutes). The addition of TBA·Br was followed by recrystallization from acetonitrile. Several sets of reaction (1-2, 0.14-0.18) yielded blue precipitates where single crystals that are suitable for X-ray diffraction analysis were obtained from reaction (1, 0.14). Figure 5 shows the structure of the resulting cluster anion and diagram. The cluster comprises 18 Mo ions templated internally with two  $SO_3^{2-}$  anions, resembling a  $\{S_2Mo_{18}\}$ , however, the outer shell is coordinated by four  $PhPO_3^{2-}$  anions which are attached to the cluster surface through Mo-O-P bonds and a sodium ion is encapsulated within the cluster. UV-vis-NIR spectra show IVCT bands at 688 and 1050 nm, indicating a mixed valence state between  $Mo^V$  and  $Mo^VI$  (figure S6-1). Redox titrations (figure S7-4) reveal that four of the 18 Mo are reduced to  $Mo(V)$  and the cluster can be formulated as:  $(TBA)_5[Na(SO_3)_2(PhPO_3)_4Mo^V_4Mo^VI_{14}O_{49}] \cdot nMeCN$  (**1**) ( $2 \geq n$ ).

A reaction of acidified molybdate with the  $S_2O_4^{2-}$  reductant yields a MB-wheel cluster at low pH and  $R$ . However, with increasing pH and  $R$ , the reaction gives a mix-

ture of building blocks containing  $\text{SO}_3^{2-}$ . As the pH or  $R$  value increases, the concentration of  $\text{SO}_3^{2-}$  and  $\text{Mo}^{\text{V}}$  in the reaction system also increases (the  $\text{SO}_3^{2-}$  forms as a result of the oxidation of the reductant  $\text{S}_2\text{O}_4^{2-}$ ).

Since  $\text{SO}_3^{2-}$  is not fully utilized as a template in the initial reaction system, treatment by TBA and acetonitrile triggers a reaction to several types of cluster anion with  $\text{SO}_3^{2-}$  anion serving as a template (Figure 6). This is illustrated by an enhancement of reactivity of the template and an encapsulation/association or ‘shrink-wrapping’ effect. In this respect we feel these findings will lead to new methodologies for new cluster design. Further, the use of other phosphonate anions substituted with a functional organic moiety will be reported by us with details on structure and electronic state of compound **1**.

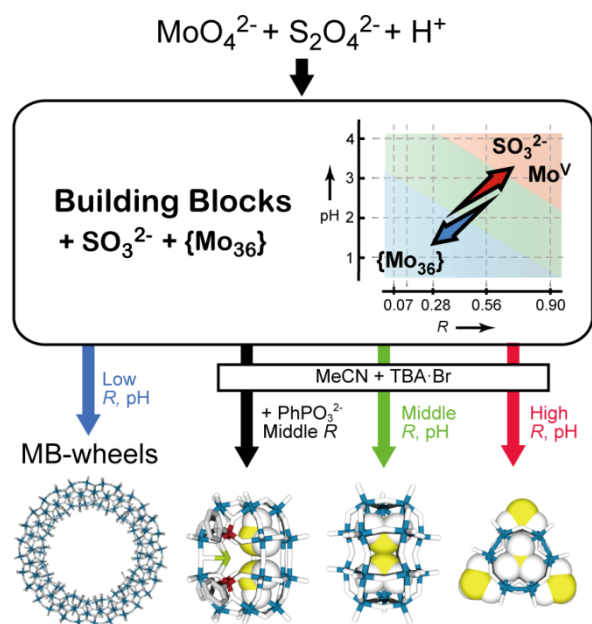


**Figure 6.** Schematic view of reaction system. S (yellow) and O (white) atoms of  $\text{SO}_3^{2-}$  were emphasized by large ball representations. Blue and white sticks were corresponded to Mo and O atoms, respectively.

### 3. CONCLUSIONS

We have investigated the self-assembly process of MB  $\{\text{Mo}_{154}/152\}$  wheels under a range of different reaction conditions, pH (1–4) and ratio of the starting materials ( $R$ ; 0.07–0.90). UV–vis–NIR spectroscopy, gel electrophoresis, and ESI-MS not only helped us to map the reaction coordinates of the  $\text{Mo}/\text{Na}_2\text{S}_2\text{O}_4$  system but also to define the areas that favor the formation of MB and Mo-brown species. We were also able to identify the available building blocks in the reaction mixtures based on the experimental variables (pH and  $R$ ). Moreover, it was shown that not only MB wheels but also other cluster anions were present in the reaction mixtures at high pH and  $R$  values. These species were isolated by addition of TBA and acetonitrile in the aqueous reaction mixture forming  $[\text{Mo}_2\text{Mo}_6\text{V}_6\text{O}_{54}(\text{SO}_3)_2]^{6-}$  and  $[(\mu_6\text{-SO}_3)\text{Mo}_6\text{V}_6\text{O}_{15}(\mu_2\text{-SO}_3)_3]^{8-}$  clusters revealing a relationship between theas-

sembled architecture and the Lewis basicity of the anionic species, the extent of the reduction, and the polarity of the solvent. The interplay of template-based and redox triggered self-assembly was tested further by the cooperative effect of sulfite and phenylphosphonate anions in a mixed solvent system, in which we isolated a new molecular capsule templated by the sulphite anions and that has an external surface decorated with four phosphonate ligands. Consequently the template driven self-assembly is favored by: (a) strong Lewis basicity of the oxoanion, (b) low oxidation state of Mo, and (c) reduced polarity of the solvent used. Our results shown here demonstrate a new design approach for the synthesis of novel clusters and the control of template triggered self-assembly.

## 4. EXPERIMENTAL PROCEDURES

### 4.1 Measurements

IR spectra ( $4000\text{--}450\text{ cm}^{-1}$ ) measurements were carried out on KBr disks with a resolution of  $4\text{ cm}^{-1}$ . All spectra are shown in supporting information (SI). Single-crystal XRD analysis was performed using Rigaku Mercury CCD area detector with graphite-monochromated  $\text{Mo-K}\alpha$  radiation. The data were collected at 173 K to a maximum  $2\theta$  value of 55.0. The structure was determined by direct methods and expanded using Fourier techniques.

### 4.2 Reactions

Aqueous solution of sodium molybdate (12.7 mmol, 25 mL) and sodium dithionite were reacted at different molar ratios to molybdate denoted as  $R = [\text{S}_2\text{O}_4^{2-}]/[\text{MoO}_4^{2-}]$  (0.07, 0.14, 0.23, 0.56 or 0.9) and solution pH was controlled by the addition of hydrochloric acid to pH 1, 2, 3 or 4. After one day of reaction in the closed flask, filtrates (solution-I) were characterized by UV-vis-NIR spectra, gel-electrophoresis and mass spectrometry.

### 4.3 Isolation from Reaction Mixture by Cation Exchange Reaction

**4.3.1 Ammonium salt.** Solution-I was treated with ammonium chloride. Single crystals were obtained from reactions (pH,  $R$ ) = (3, 0.07–0.14). The cluster type was crystallographically identified as  $[\text{Mo}_{138}\text{O}_{410}(\text{OH})_{20}(\text{H}_2\text{O})_{46}]^{40-}$ .

**4.3.2 TEAH salt.** A similar procedure with triethanolammonium (TEAH) chloride (1.0 g) gave blue precipitates from solution-I. They were characterized by using IR spectroscopy to determine cluster type. The TEAH salt showed spectra typical for MB-wheels shown in SI. A filtrate (solution-II) after separating TEAH salt was characterized using gel-electrophoresis which showed that the blue band that had slowest mobility was diminished if compared with that of solution-I.

**4.3.3 TBA salt.** Solution-II was treated with tetrabutylammonium (TBA) bromide (1.0 g), yielding an immediate precipitate depending on reaction conditions. The TBA salt was recrystallized from acetonitrile giving single crystals suitable for XRD analysis and IR spectra were collected in addition (see ESI figure S4-6 to S4-10). They were identified to  $\{\text{S}_2\text{Mo}_8\}$ . If the filtrates were orange in color, single crystals could be obtained after 5–7

days by keeping flask opened. Single crystal XRD analysis and IR spectra (figure S4-11 to S4-12) revealed that  $\{S_4Mo_6\}$  anion included in the crystal.

#### 4.4 Gel-electrophoresis

The electrophoresis studies were performed using a commercially available submarine-type electrophoresis system (Pt-wire electrodes set at a distance of 13 cm). Acetic acid/sodium acetate buffer (pH 5.0) was applied and agarose (purchased from Sigma Aldrich and used without further purification) gels were prepared using the same buffer by cooling an agarose solution from boiling temperature. A solution was injected into slots in the gels in 15  $\mu$ L portions and a voltage (100 V) was applied to the system for 10 min.

#### 4.5 Characterization of $\{S_2Mo_{18}\}$ anion

The cluster type have been reported so far,<sup>12</sup> while we isolated as a TBA salt. From XRD analysis, redox titration, IR and UV-vis-NIR spectroscopy, composition was suggested as  $TBA_5H[Mo_2^V Mo^{VI}_{16}O_{54}(SO_3)_2] \cdot 3MeCN$ . The crystalline products were collected by filtration, and dried to remove acetonitrile for elemental analysis. (Found: C, 24.48; H, 4.64; N, 1.95; Calc for  $C_{80}H_{181}Mo_{18}N_5O_{60}S_2$ : C, 24.24; H, 4.60; N, 1.77 %). UV-vis-NIR spectra (acetonitrile) :  $\lambda_{max}(MeCN)/nm$  801 ( $\epsilon/dm^3 mol^{-1} cm^{-1}$  8032) Crystal data for  $\{S_2Mo_{18}\}$  anion:  $C_{84.5}H_{186}Mo_{18}N_{7.5}O_{60}S_2$ ,  $M = 4058.45 g mol^{-1}$ , orthorhombic,  $a = 18.0117(2)$ ,  $b = 27.2840(5)$ ,  $c = 28.0044(5) \text{ \AA}$ ,  $V = 13762.2(4) \text{ \AA}^3$ ,  $T = 173 K$ , space group  $P2_12_12_1$ (no. 19),  $Z = 4$ , 147665 reflections measured, 31543 unique ( $R_{int} = 0.0506$ ) which were used in all calculations. The final  $R_1$  (observed data) and  $wR_2$  (all data) were 0.0666 and 0.1924, respectively. CCDC number 1037251.

#### 4.6 Characterization of $\{S_4Mo_6\}$ anion

The anion also has been reported with different counter cations.<sup>13</sup> The orange crystals turned opaque easily due to desorption of crystalline water however we were able to solved the crystal structure revealing the compound as  $[(\mu_6-SO_3)Mo^V_6O_{15}(\mu_2-SO_3)_3]^{8-}$ , a cluster anion with several TBA cations, disordered water molecules and sodium ion. Crystallographic data and IR spectra were included in SI.

#### 4.7 Synthesis and characterization of **1**.

Single crystals of the compound **1** were obtained by following procedure. The reaction variable is corresponded to (1, 0.18). To an aqueous solution of  $Na_2MoO_4 \cdot 2H_2O$  (12.6 mmol, 25 mL) was added, hydrochloric acid (32 %, 3.0 mL),  $Na_2S_2O_4$  (2.30 mmol), phenylphosphonic acid (3 mmol) and acetonitrile (10 mL) under continuous stirring for 30 min (pH 1 before adding acetonitrile) and the filtrate was kept in a closed flask for three days. After filtration, TBA-Br (0.70 g) was added and a blue precipitation was formed which was then recrystallized from acetonitrile. Blue crystals were obtained after 2-3 days. Redox titration with  $Ce^{IV}(SO_4)_2$  (0.01 N) in mixed solvent (DMSO; 5 ml, 1 M  $H_2SO_4$ ; 5 ml) showed that there are four equivalent numbers of  $Mo^V$ . Composition was deduced to  $(TBA)_5[Na(SO_3)_2(PhPO_3)_4 Mo^V_4 Mo^{VI}_{14}O_{49}] \cdot nMeCN$  (two acetonitrile molecules are identified crystallographically,

however it still contains space for uncertain solvent molecule). Yield: 1.83 g (42 % based on Mo). Elemental analysis: Found: C, 27.48; H, 4.20; N, 1.48; Calculated for  $C_{104}H_{200}Mo_{18}N_5NaO_{67}P_4S_2$ : C, 27.57; H, 4.45; N, 1.55 %. UV-vis-NIR spectra (acetonitrile) :  $\lambda_{max}(MeCN)/nm$  668, 1050. IR (KBr):  $\nu_{max}/cm^{-1}$  3446 (br), 2961 (m), 2873 (m), 2360 (w), 1635 (w), 1482 (m), 1380 (w), 1184 (m), 1146 (m), 1133 (m), 1045 (m), 1026 (m), 963 (s), 937 (s), 909 (m), 867 (w), 816 (m), 788 (m), 724 (m), 708 (m), 562 (m) (see figure S4-13). Crystal data for **1**:  $C_{56}H_{89}Mo_9N_{4.5}Na_{0.5}O_{33.5}P_2S$ ,  $M = 2330.27 g mol^{-1}$ , monoclinic,  $a = 33.20(2)$ ,  $b = 17.635(10)$ ,  $c = 32.189(20) \text{ \AA}$ ,  $\beta = 115.3192(18)^\circ$ ,  $V = 17033(17) \text{ \AA}^3$ ,  $T = 173 K$ , space group  $C2/c$  (no. 15),  $Z = 8$ , 61365 reflections measured, 17768 unique ( $R_{int} = 0.1516$ ) which were used in all calculations. The final  $R_1$  (observed data) and  $wR_2$  (all data) were 0.0885 and 0.2571, respectively. CCDC number 1037252.

## ASSOCIATED CONTENT

**Supporting Information.** UV-vis-NIR spectra, chromatographic gel-electrophoresis, isolation and identification of MB-wheels, IR analysis, mass spectra, redox titration, structural data including CIF files, Lewis base strength from bond valence consideration and reaction scanning for compound **1**. This material is available free of charge via the Internet at <http://pubs.acs.org>.

## AUTHOR INFORMATION

### Corresponding Authors

\* Ryo Tsunashima (ryotsuna@yamaguchi-u.ac.jp) and Leroy Cronin (Lee.Cronin@glasgow.ac.uk)

## ACKNOWLEDGMENT

This work was partly supported by the Grant-in-Aid for Science Research from the Ministry of Education, Culture, Sports, Science and Technology of Japan. We thank the EPSRC platform grant (No. EP/J015156/1) and programme grant (No. EP/L023652/1). LC thanks the Royal Society / Wolfson Foundation for a Merit Award and we also would like to thank the University of Glasgow for funding.

## REFERENCES

- (1) (a) Müller, A.; Meyer, J.; Krickemeyer, E.; Diemann, E. *Angew. Chem., Int. Ed. Engl.*, **1996**, 35, 1206–1208. (b) Müller, A.; Roy, S. *Coord. Chem. Rev.*, **2003**, 245, 153–166. (c) Müller, A.; Serain, C. *Acc. Chem. Res.*, **2000**, 33, 2–10. (d) Baker, L. C. W.; Glick, D. C. *Chem. Rev.*, **1998**, 98, 3–49.
- (2) (a) Song, Y.-F.; Tsunashima, R. *Chem. Soc. Rev.*, **2012**, 41, 7384–7402. (b) Long, D.-L.; Tsunashima R.; Cronin, L. *Angew. Chem., Int. Ed.*, **2010**, 49, 1736–1758.
- (3) Müller, A.; Das, S. K.; Fedin, V. P.; Krickemeyer, E.; Beugholt, C.; Bögge, H.; Schmidtman, M.; Hauptfleisch, B. *Z. Anorg. Allg. Chem.*, **1999**, 625, 1187–1192.
- (4) (a) Liu, T.; Diemann, E.; Li, H.; Dress, A.W. M.; Müller, A. *Nature*, **2003**, 426, 59–62. (b) Liu, T. *Langmuir*, **2010**, 26, 9202–9213.
- (5) (a) Noro, S.; Tsunashima, R.; Kamiya, Y.; Uemura, K.; Kita, H.; Cronin, L.; Akutagawa, T.; Nakamura, T. *Angew. Chem., Int. Ed.*, **2009**, 48, 8703–8706. (b) Imai, H.; Akutagawa, T.; Kudo, F.; Ito, M.; Toyoda, K.; Noro, S.; Cronin, L.; Nakamura, T. *J. Am. Chem. Soc.*, **2009**, 131, 13578–13579. (c) Tsuda, A.; Hirahara, E.; Kim, Y.-S.; Tanaka, H.; Kawai, T.; Aida, T. *Angew. Chem., Int. Ed.*,

- 2004, 43, 6327–6331. (d) Alam, M. A.; Kim, Y.-S.; Ogawa, S.; Tsuda, A.; Ishii, N.; Aida, T. *Angew. Chem., Int. Ed.*, **2008**, 47, 2070–2073. (e) Polarz, S.; Smarsly, B.; Antonietti, M. *ChemPhysChem*, **2001**, 2, 457–461.
- (6) (a) Miras, H. N.; Cooper, G. J. T.; Long, D.-L.; Bögge, H.; Müller, A.; Streb, C.; Cronin, L. *Science*, **2010**, 327, 72–74. (b) Miras, H. N.; Richmond, C. J.; Long, D.-L.; Cronin, L. *J. Am. Chem. Soc.*, **2012**, 134, 3816–3824.
- (7) Tsunashima, R.; Richmond, C.; Cronin, L. *Chem. Sci.*, **2012**, 3, 343–348.
- (8) Müller, A.; Merca, A.; Al-Karawi, A. J. M.; Garai, S.; Bögge, H.; Hou, G.; Wu, L.; Haupt, E. T. K.; Rehder, D.; Haso, F.; Liu, T. *Chem.–Eur. J.*, **2012**, 18, 16310–16318.
- (9) Müller, A.; Krickemeyer, E.; Bögge, H.; Schmidtman, M.; Beugholt, C.; Das, S. K.; Peters, F. *Chem.–Eur. J.*, **1999**, 5, 1496–1502.
- (10) Shishido, S.; Ozeki, T. *J. Am. Chem. Soc.*, **2008**, 130, 10588–10595.
- (11) (a) Wilson, E. F.; Abbas, H.; Duncombe, B. J.; Streb, C.; Long, D.-L.; Cronin, L. *J. Am. Chem. Soc.*, **2008**, 130, 13876–13884. (b) Rosnes, M. H.; Yvon, C.; Long, D.-L.; Cronin, L. *Dalton Trans.*, **2012**, 41, 10071–10079.
- (12) Long, D.-L.; Kögerler, P.; Cronin, L. *Angew. Chem., Int. Ed.*, **2004**, 43, 1817–1820.
- (13) Manos, M. J.; Woollins, J. D.; Slawin, A. M. Z.; Kabanos, T. A. *Angew. Chem., Int. Ed.*, **2002**, 41, 2801–2805.
- (14) Pradeep, C. P.; Long, D.-L.; Cronin, L. *Dalton Trans.*, **2010**, 39, 9443–9457.
- (15) Fielden, J.; Quasdorf, K.; Cronin, L.; Kögerler, P. *Dalton Trans.*, **2012**, 41, 9876–9878.
- (16) Brown, I. D. in *Structure and Bonding in Crystals*; O’Keeffe, M., Navrotsky, A., Eds.; Academic Press: New York, 1981; Vol. 2, pp 1–30.
- (17) (a) Woods, J. T.; Mellon, M. G. *Ind. Eng. Chem., Anal. Ed.*, **1941**, 13, 760–764. (b) Clausen, D. F.; Shroyer, J. H. *Anal. Chem.*, **1948**, 20, 925–926.
- (18) Strickland, J. D. H. *J. Am. Chem. Soc.*, **1952**, 74, 862–867.
- (19) Deltcheff, C. R.; Fournier, M.; Franck, R.; Thouvenot, R. *Inorg. Chem.*, **1983**, 22, 207–216.
- (20) Ichida, H.; Sasaki, Y. *Acta Crystallogr., Sect. C: Struct. Chem.*, **1983**, 39, 529–533.
- (21) Himeno, S.; Saito, A.; Hori, T. *Bull. Chem. Soc. Jpn.*, **1990**, 63, 1602–1606.
- (22) Corella-Ochoa, M. N.; Miras, H. N.; Long, D.-L.; Cronin, L. *Chem.–Eur. J.*, **2012**, 18, 13743–13754.
- (23) Gao, J.; Yan, J.; Beeg, S.; Long, D.-L.; Cronin, L. *Angew. Chem., Int. Ed.*, **2012**, 51, 3373–3376.
- (24) Long, D.-L.; Abbas, H.; Kögerler, P.; Cronin, L. *Angew. Chem., Int. Ed.*, **2005**, 44, 3415–3419.
- (25) (a) Hori, T.; Tamada, O.; Himeno, S. *J. Chem. Soc., Dalton Trans.*, **1989**, 1491–1497. (b) Hori, T.; Himeno, S.; Tamada, O. *J. Chem. Soc., Dalton Trans.*, **1996**, 2083–2087. (c) Müller, A.; Botar, B.; Das, S. K.; Bögge, H.; Schmidtman, M.; Merca, A. *Polyhedron*, **2004**, 23, 2381–2385.
- (26) Zhu, S.-S.; Yue, B.; Shi, X.-Q.; Gu, Y.-D.; Liu, J.; Chen, M.-Q.; Huang, Y.-F. *J. Chem. Soc., Dalton Trans.*, **1993**, 3633–3634.
- (27) (a) Kolthoff, I. M. *Treatise on Analytical Chemistry*; Interscience Encyclopedia, Inc.: New York, 1959. (b) Brownstein, S.; Stillman, A. E. *J. Phys. Chem.*, **1959**, 63, 2061–2062. (c) Hildebrand, J. H. *Principles of Chemistry*; The Macmillan Company: New York, 1940. (d) Bjerrum, J.; Schwarzenbach, G.; Sillen, L. G. *Stability Constants*; Chemical Society: London, 1958. (e) Cruywagen, J. J. *Adv. Inorg. Chem.*, **1999**, 49, 127–182.
- (28) Nagarajan, K.; Shelly, K. P.; Perkins, R. P.; Stewart, R. *Can. J. Chem.*, **1987**, 65, 1729–1733.

TOC figure

